BEAM DYNAMICS FOR A HIGH FIELD C-BAND HYBRID PHOTOINJECTOR*

L. Faillace[†1], F. Bosco[2], M. Carillo[2], L. Giuliano[2], M. Migliorati[2], A. Mostacci[2], L. Palumbo[2]
Sapienza University, Rome, Italy
R. Agustsson, I. Gadjev, S. Kutsaev, A. Murokh, RadiaBeam Systems, Santa Monica, CA, USA
M. Behtouei, A. Giribono, B. Spataro, C. Vaccarezza, INFN/LNF, Frascati, Italy
A. Fukasawa, N. Majernik, O. Williams, J. B. Rosenzweig
University of California, Los Angeles, CA, USA
S. Tantawi, SLAC National Accelerator Laboratory, Menlo Park, CA, USA
[1]also at INFN/LNF, Frascati, Italy
[2]also at INFN/Roma1, Rome, Italy

Abstract

In this paper, we present a new class of a hybrid photoinjector in C-Band. This project is the effort result of a UCLA/Sapienza/INFN-LNF/RadiaBeam collaboration. This device is an integrated structure consisting of an initial standing-wave 2.5-cell gun connected to a traveling-wave section at the input coupler. Such a scheme nearly avoids power reflection back to the klystron, removing the need for a high-power circulator. It also introduces strong velocity bunching due to a 90° phase shift in the accelerating field. A relatively high cathode electric field of 120 MV/m produces a 4 MeV beam with ~ 20 MW input RF power in a small foot-print. The beam transverse dynamics are controlled with a ~ 0.27 T focusing solenoid. We show the simulation results of the RF/magnetic design and the optimized beam dynamics that shows 6D phase space compensation at 250 pC. Proper beam shaping at the cathode yields a 0.5 mm-mrad transverse emittance. A beam waist occurs simultaneously with a longitudinal focus of < 400 fs rms and peak current >600 A. We discuss application of this injector to an Inverse-Compton Scattering system and present corresponding start-to-end beam dynamics simulations.

INTRODUCTION

Existing and recently proposed linear accelerator-based facilities, such as electron-positron or photon colliders, X-ray free-electron lasers [1], wake-field accelerators, coherent THz and inverse Compton scattering X-ray or γ-ray sources [2], demand electron beams with high peak currents and ultra-low normalized emittances. Electron beams with these parameters'combination, usually referred to as high beam brightness, will unravel new research scenarios for users with applications not only for high-energy physics but also in medicine where low emittance photon beams are necessary to obtain high quality in images for diagnostics, because it will increase the resolution and contrast.

In the state-of-art of photoinjectors worldwide, the basic layout consists of a standing-wave (SW) radio-frequency

(RF) structure, usually referred to as the RF gun, and usually one travelling-wave (TW) linac. The electron beam is generated at the surface of the cathode plate located in the first accelerating cell of the RF gun. The bunch is extracted via photoelectric effect by typically using an IR laser pulse. Inside the RF gun, the electrons become fairly relativistic (i.e. up to 4-5 MeV) and, after balistically propagate through a drift tube, are then injected into the TW linac for further required energy gain. The drift tube length is properly chosen in order for the beam to undergo the emittance compensation process [3]. Typical lengths of this beam pipe are of the order of 1.5 m in S-band. Since the RF input power into the gun and the linac is either fed indipendently or by one single klystron with the use of a power splitter, there is need for a circulator located upstream the waveguide network connected to the SW gun in order to protect the power source from inevitable reflections.
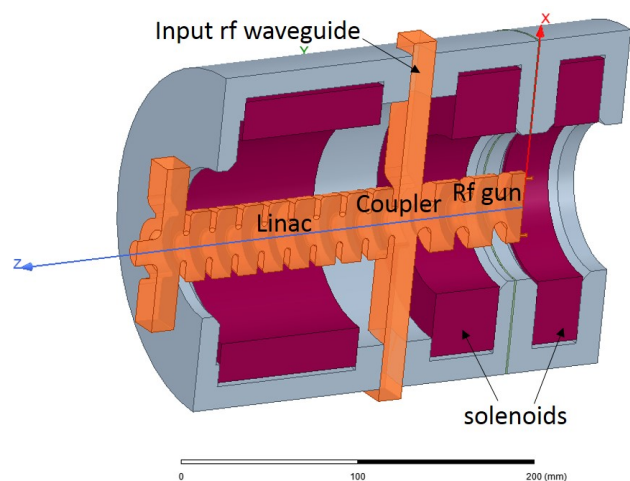

Figure 1: Basic layout of the compact hybrid C-band photoinjector.

The design of a compact hybrid photoinjector which effectively combines the two RF structures into one, eliminating the beam tube and removing the need for the circulator. The basic scheme (i.e. SW gun and TW linac) is unchanged, but a cell that couples the two structures directly replaces

MC2: Photon Sources and Electron Accelerators

A08 Linear Accelerators

the long beam pipe and matching section. The coupler cell, which acts as a matching network, has a double function: it is the first cell of the TW section, and the coupler cell of the whole photoinjector, since the total input RF power is coupled through it. The first hybrid photo-injector was carried out in S-Band by UCLA in collaboration with INFN-LNF. The RF design and beam-dynamics design can be found in [4]. The high-power tests were carried out at Pegasus Lab, UCLA [5], with an RF power up to 11.5 MW from the klystron. The frequency scaling of this design was analyzed in [6], showing easy implementation and scaling to higher frequencies. As a matter of fact, with this information in hand, the X-band version of the photoinjector was produced [7] as well as the beam dynamics simulations [8].

In this paper, we propose the design of the hybrid photo-injector working in C-band at 5.712 GHz as a compromise between S- and X-band options. Operating at higher frequencies, with respect to the S-band version, makes it a more compact structure and gives the possibility of high brightness beams, proportional to λ^{-2}. On the other hand, working at a lower RF frequency, compared with the X-band case, the whole system is more cost-effective, especially from the RF power source point of view. It is the first time we also perform the whole emittance compensation process optimization for this class of photo-injector. In Fig. 1 is shown the basic layout of the compact hybrid C-band photo-injector. The main advantages of this new configuration are as follows:

- Reduced initial RF mismatch, i.e. low reflected power, between the source the structure;
- RF power is provided only through one waveguide, and no circulator is needed;
- Considerably reduced RF and accelerator system footprint;
- Enabling the scaling to C-band allows exploitation of the natural scaling of photoinjector brightness [9] with RF wavelength, i.e. $B_e = 2I/\epsilon_n^2 \sim \lambda^{-2}$;
- Possibility of obtaining ultra-short electron bunches due to velocity bunching (VB) between the SW and TW sections (as discussed in the following Section).

In the following sections, we will discuss the RF and beam dynamics of the C-band hybrid photoinjector. We also addressed the unique beam envelope dynamics and the wakefield effects inside this structure and can be found in [10] and [11], respectively.

RF DESIGN

The RF design of the compact photoinjector was carried out in HFSS [12]. One quarter section of the C-band hybrid photoinjector from HFSS is shown in Fig. 2.

The on-axis accelerating electric field can be expressed as follows:

$$E_z(z,t) = E_0(z) \cos(\varphi(z) + \omega t), \qquad (1)$$

where $E_0(z)$ is the on-axis field amplitude and $\varphi(z)$ the field phase.
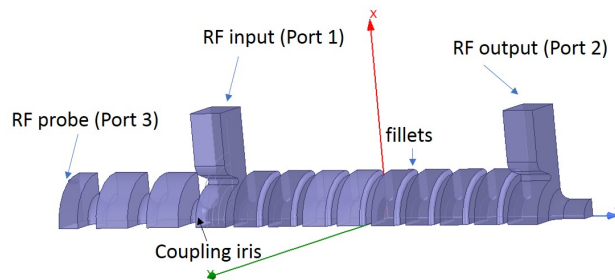
Figure 2: One quarter section of the C-band hybrid photoinjector from HFSS.

The on-axis electric field amplitude profile and phase distribution are shown in Figs. 3 and 4, respectively. The $\pi/2$ phase-shift between the SW and TW section, a particular feature of this hybrid structure, allows for velocity bunching thus obtaining ultra-short beams.
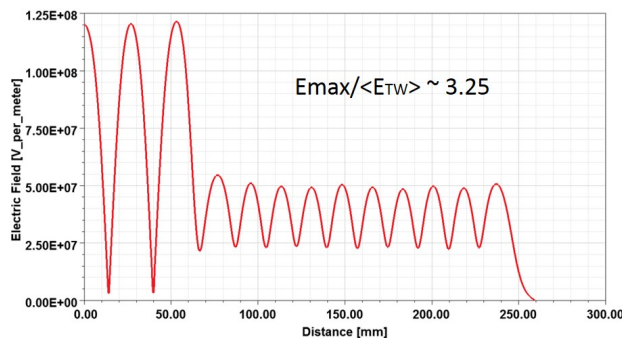

Figure 3: On-axis electric field amplitude profile.
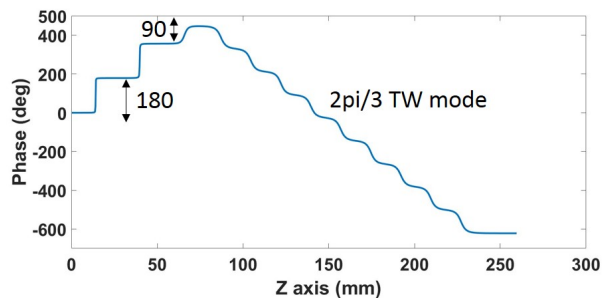

Figure 4: On-axis electric field phase distribution.

BEAM DYNAMICS

The beam dynamics of the C-band photoinjector was performed by using the General Particle Tracer (GPT) code [13]. The main input electron beam parameters at the extraction (cathode) are given in Table 1. The beam charge is Q= 250 pC. The rms spot size is $\sigma_{x,y}$= 500 μm with a gaussian distribution cut a 1σ. The bunch length is also gaussian with σ_z= 0.5 ps.

The on-axis normalized magnetic field profile is given in Fig. 5. The optimal peak magnetic field of the solenoid around the hybrid structure is B_z= 0.27 T. A bucking coil is used to cancel out the magnetic field at the cathode.

Table 1: Main Input Electron Beam Parameters

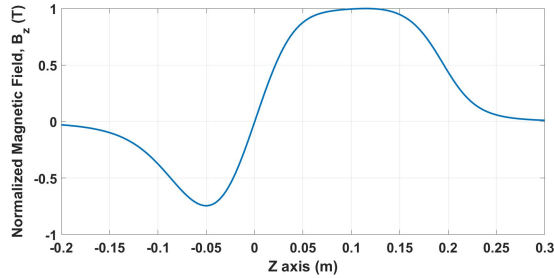| Parameter	Value
Beam Charge, Q	250 pC
Spot Size, $\sigma_{x,y}$ (cut at 1 σ)	0.5 mm
Bunch Length, σ_z	0.5 ps
E-field at cathode, E_0	120 MV/m
Number of macro-particles	50 000

Figure 5: On-axis normalized magnetic field profile.

Two linacs based on a distributed-coupling geometry proposed by Sami Tantawi, operated at 50 MV/m accelerating gradient, are used. The first linac is located at 80 cm from the hybrid photoinjector. The beam energy gain up to 100 MeV is given in Fig. 6.
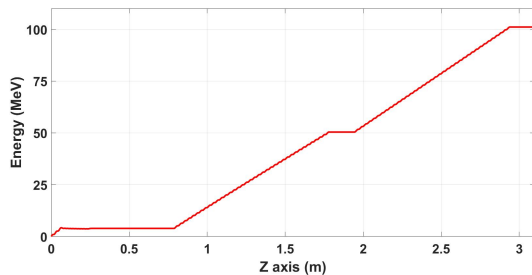

Figure 6: The beam energy gain from the cathode at z= 0m up to the exit of the second linac.

All parameters were finalized in order to obtain the beam emittance minimization to ϵ_n= 0.5 mm-mrad, as shown in Fig. 7 and a bunch compression down to σ_z= 400 fs (see Fig. 8), corresponding to a beam peak currrent above 600 A. This results in the 6D phase space (both on the transverse and longitudinal planes) compensation.

CONCLUSIONS

We have presented the RF and beam dynamics optimization analysis of a new class of a hybrid (SW/TW) photoinjector in C-Band. This design is the extension and evolution for this new class of device.

We have optimized the SW and TW sections in order to obtain 120 MV/m at the cathode with < 20 MW RF input power. The detailed beam dynamics analysis was carried out first in order to find the operational values of the photoinjector, such as the solenoid magnetic field, for the emittance
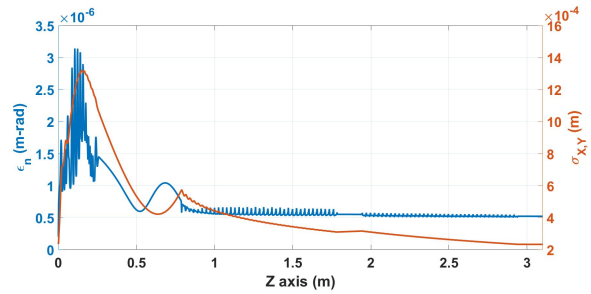
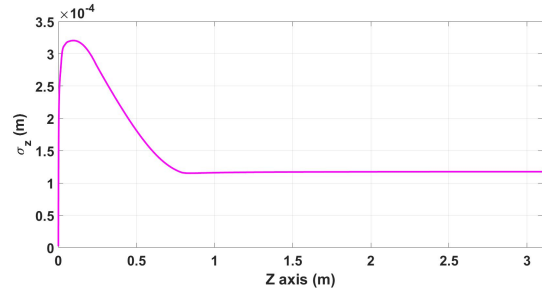Figure 7: Evolution of the beam normalized transverse emittance along the beamline.

Figure 8: Evolution of the beam normalized longitudinal emittance along the beamline.

compensation process. Secondly, by properly inserting two downstream linacs, with relatively high accelerating gradient (50 MV/m), it was possible to achieve the 6D phase space compensation (both on the transverse and longitudinal planes) with a 250 pC electron bunch. A proper beam shaping at the cathode yields a 0.5 mm-mrad transverse emittance. The beam waist occurs simultaneously with a longitudinal focus of < 400 fs rms and a peak current > 600 A.

In particular, as a specific application, we have successfully investigated the operation with two 50 MV/m linacs for an ICS source. It has to be pointed out that our proposed hybrid structure can also serve as the photoinjector for an FEL. Finally, we want to highlight that this hybrid structure is suitable for cryogenics operation, thus higher accelerating gradients can be obtained.

REFERENCES

[1] J. B. Rosenzweig *et al.*, "Next generation high brightness electron beams from ultrahigh field cryogenic RF photocathode sources", *Physical Review Accelerators and Beams*, vol. 22, no. 2, p. 023403, 2019. doi:10.1103/physrevaccelbeams.22.023403

[2] L. Faillace *et al.*, "Status of compact inverse Compton sources in Italy: BriXS and STAR", in *Proc. SPIE 11110, Advances in Laboratory-based X-Ray Sources, Optics, and Applications VII*, San Diego, CA, USA, Sep. 2019. doi:10.1117/12.2531168

[3] L. Serafini and J. B. Rosenzweig, "Envelope analysis of intense relativistic quasilaminar beams in rf photoinjectors: mA theory of emittance compensation", *Physical Review E*, vol. 55, no. 6, pp. 7565–7590, Jun. 1997. doi:10.1103/physreve.55.7565

[4] B. O'Shea *et al.*, "RF Design of the UCLA/INFN Hybrid SW/TW Photoinjector", *AIP Conference Proceedings*, vol. 877, pp. 873–879, 2006. `doi:10.1063/1.2409228`

[5] B. O'Shea *et al.*, "Measurement of the UCLA/URLS/INFN Hybrid Gun", in *Proc. 22nd Particle Accelerator Conf. (PAC'07)*, Albuquerque, NM, USA, Jun. 2007, paper WEPMS035, pp. 2418-2420.

[6] A. Fukasawa *et al.*, "Charge and Wavelength Scaling of the UCLA/URLS/INFN Hybrid Photoinjector", in *Proc. 22nd Particle Accelerator Conf. (PAC'07)*, Albuquerque, NM, USA, Jun. 2007, paper THPAS052, pp. 3609-3611.

[7] B. Spataro *et al.*, "RF properties of a X-band hybrid photoinjector", *Nuclear Instruments and Methods in Physics Research Section A: Accelerators, Spectrometers, Detectors and Associated Equipment*, vol. 657, pp. 99-106, 2011. `doi:10.1016/j.nima.2011.04.057`

[8] J. B. Rosenzweig *et al.*, "Design and applications of an x-band hybrid photoinjector", *Nuclear Instruments and Methods in Physics Research Section A: Accelerators, Spectrometers, Detectors and Associated Equipment*, vol. 657, pp. 107-113, 2011. `doi:10.1016/j.nima.2011.05.046`

[9] J. B. Rosenzweig and E. Colby, "Charge and wavelength scaling of RF photoinjector designs", *AIP Conference Proceedings*, vol. 335, no. 1, pp. 724-737, 1995. `doi:10.1063/1.48260`

[10] M. Carillo *et al.*, "Three-Dimensional Space Charge Oscillations in a Hybrid Photoinjector", presented at the 12th Int. Particle Accelerator Conf. (IPAC'21), Campinas, Brazil, May 2021, paper WEPAB256, this conference.

[11] F. Bosco *et al.*, "Modeling Short Range Wakefield Effects in a High Gradient Linac", presented at the 12th Int. Particle Accelerator Conf. (IPAC'21), Campinas, Brazil, May 2021, paper WEPAB238, this conference.

[12] Ansys HFSS, `https://www.ansys.com/products/electronics/ansys-hfss`

[13] Pulsar Physics, `http://www.pulsar.nl/gpt/index.html`